AIP | Applied Physics Letters

# InAs/AlAsSb based quantum cascade detector

Peter Reininger, Tobias Zederbauer, Benedikt Schwarz, Hermann Detz, Donald MacFarland, Aaron Maxwell Andrews, Werner Schrenk, and Gottfried Strasser

Citation: Applied Physics Letters **107**, 081107 (2015); doi: 10.1063/1.4929501
View online: http://dx.doi.org/10.1063/1.4929501
View Table of Contents: http://scitation.aip.org/content/aip/journal/apl/107/8?ver=pdfcov
Published by the AIP Publishing



# InAs/AlAsSb based quantum cascade detector

Peter Reininger,[1,a)] Tobias Zederbauer,[1] Benedikt Schwarz,[1] Hermann Detz,[2] Donald MacFarland,[1] Aaron Maxwell Andrews,[1] Werner Schrenk,[1] and Gottfried Strasser[1]
[1]*Institute for Solid State Electronics and Center for Micro- and Nanostructures, TU Wien, Floragasse 7, 1040 Vienna, Austria*
[2]*Austrian Academy of Sciences, Dr. Ignaz Seipel-Platz 2, 1010 Vienna, Austria*

(Received 8 June 2015; accepted 12 August 2015; published online 24 August 2015)

In this letter, we introduce the InAs/AlAsSb material system for quantum cascade detectors (QCDs). InAs/AlAsSb can be grown lattice matched to InAs and exhibits a conduction band offset of approximately 2.1 eV, enabling the design of very short wavelength quantum cascade detectors. Another benefit using this material system is the low effective mass of the well material that improves the total absorption of the detector and decreases the intersubband scattering rates, which increases the device resistance and thus enhances the noise behavior. We have designed, grown, and measured a QCD that detects at a wavelength of $\lambda = 4.84\,\mu$m and shows a peak specific detectivity of approximately $2.7 \times 10^7$ Jones at $T = 300$ K.  [http://dx.doi.org/10.1063/1.4929501]

Quantum cascade detectors (QCDs) are intersubband photodetectors whose properties are determined by quantum engineering and thus provide a vast design and optimization freedom. Since the first demonstration of the QCD, people worked to optimize the detector performance, as well as to extend its detection frequency range.[1–7] So far, detection has been demonstrated from the near-infrared to the THz region, but room-temperature operation with decent device performance has been reached only in the mid-infrared and near-infrared.[8–12] When aiming for higher transition energies, the material systems conduction band offset (CBO) is usually the limiting material property. To extend the detection range of QCDs, different material systems have to be explored. One of the recent material systems, where QCDs have already been demonstrated, is the II-VI based ZnCdSe and ZnCdMgSe, which provides a high CBO of up to $\Delta E_c \approx 1.1$ eV.[11] Another material with a high CBO is GaN/AlGaN, where detectors down to a wavelength of 1 $\mu$m were demonstrated.[10] Although the demonstrated II-VI or III-N based QCDs showed excellent performance in terms of specific detectivity, they exhibited a low responsivity. A reason for the low responsivity could be the high electron effective mass of $m_e \approx 0.13 m_0$ for the II-VI system and $m_e \approx 0.2 m_0$ for GaN. To explain this behaviour, we use the definition of the responsivity for QCDs, which is given by

$$R = \frac{\lambda e}{hc} \eta p_e \frac{1}{N}, \tag{1}$$

where $\eta$ is the absorption efficiency, $p_e$ is the extraction efficiency, and $N$ is the number of QCD cascades. The absorption efficiency is the probability that a photon that travels through the QCD material induces an electronic transition between the two optically active energy levels. The extraction efficiency is the probability that an excited electron escapes the active well and tunnels through the extractor into the ground level of the next cascade and thus contributes to the photocurrent. For a given doping density, the absorption coefficient of the QCD material is inversely proportional to the electron effective mass, i.e., the smaller the effective mass the larger the absorption.[2] From this perspective, a material system for short wavelength QCDs should exhibit a small effective mass combined with a sufficiently large conduction band offset.

In this letter, we introduce the InAs/AlAsSb material system for quantum cascade detectors. QCDs that are fabricated from this material system benefit from the very high conduction band offset of $\Delta E_c \approx 2.1$ eV combined with the low effective mass of InAs, which is $m_e = 0.021 m_0$.[13] Since the QCD was measured in a 45° polished facet mesa configuration, the bandgap of InAs, which is only 0.354 eV, is imposing an upper limit to the detection range. Incident radiation with an energy above the bandgap is absorbed while passing through the substrate by generating electron hole pairs. One way to improve on this limitation is by processing the device as freestanding slab[14] and using superlattice contacts to artificially increase the transition energy between states in the valence and conduction band. The conduction band diagram of the QCD we have designed, grown, and measured is depicted in Figure 1. The QCD was designed using a semi-classical Monte-Carlo transport simulator, which is part of the Vienna Schrödinger Poisson (VSP) framework.[15] In contrast to longer wavelength designs, where a diagonal transition design is more favorable, we have chosen to use a vertical transition design.[12] At such high transition energies, the scatter rate of excited electrons in the upper absorption level back to the lower absorption level is much smaller than into energetically closer extractor levels. Thus, the extraction efficiency is already large, even without a diagonal optically active transition. In fact, the most limiting factor for low wavelength detectors is the decreasing absorption coefficient. Thus, it was the goal to make the dipole matrix element as large as possible, while keeping a sufficiently large extraction efficiency. Since this

a)Electronic mail: peter.reininger@tuwien.ac.at

 

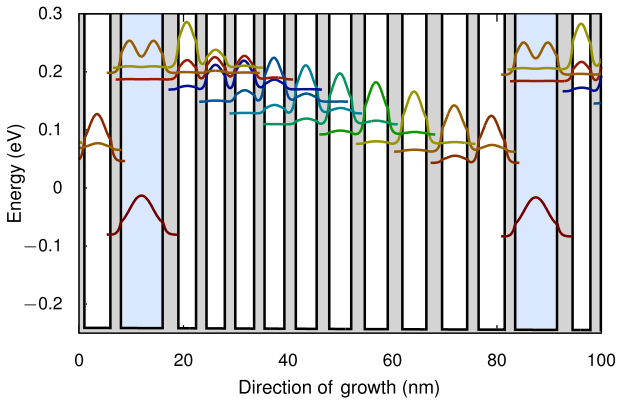


FIG. 1. The conduction band diagram of our InAs/AlAsSb QCD. The optical transition takes place between the two levels in the blue shaded well. An electron is excited from the lower to the upper state. From there, it can escape into the extractor, eventually reaching the ground level of the next cascade and contributing to the photocurrent. The device was not optimized for maximum performance, but for high robustness. The layer thicknesses in nm are **2.0**/8.0/**3.0**/3.4/**2.0**/3.5/**2.0**/3.6/**2.0**/3.8/**2.2**/4.0/**2.4**/4.2/**2.6**/4.4/**2.8**/4.6/**3.0**/4.8/**2.2**/5.0 with the underlined layer doped at $n = 4 \times 10^{17}\,\mathrm{cm}^{-3}$. The doping position is also indicated as shaded blue region. The barriers are indicated in bold.

is the first InAs/AlAsSb QCD and the growth of this material is still a challenge due to group V mixing, we aimed for high robustness against growth deviations, rather then optimum performance. This was achieved by reducing the thickness's of all barriers, and thereby increasing the coupling of the individual levels. Also, the extraction is not based on resonant coupling of two distinct states. In this design, we have two first extractor states, one energetically higher than the upper absorption level, the other one lower. This should keep a high extraction efficiency even if the layer thicknesses of the grown sample deviate from the design.

The sample was grown in a Riber molecular beam epitaxy (MBE) system on a free-standing n-InAs (001) substrate. The 30 cascades of the QCD are sandwiched between a 600 nm Si-doped InAs bottom contact layer and a 200 nm Si-doped InAs top contact layer. Before growth, the oxide was thermally desorbed at 510 °C for 20 min under an $As_2$ flux. After desorption of the oxide, a 50 nm InAs buffer layer was grown at 480 °C. The temperature was then lowered to 400 °C to grow the heterostructure. For the group V materials, valved cracking cells were used. To produce $As_2$ and $Sb_2$, the cracking zone temperatures were set to 850 °C and 1000 °C, respectively. The InAs growth rate was 0.5 $\mu$m $h^{-1}$, while AlAsSb was grown at 0.18 $\mu$m $h^{-1}$. To ensure high crystal quality, the $As_2$ pressure was calibrated using the technique described in Ref. 16. The quality of both the InAs and the AlAsSb layers was examined by Atomic Force Microscopy (AFM) on bulk samples prior to the growth of the QCD. The grown heterostructures were measured with double and triple axis high resolution X-ray diffraction (HRXRD). When growing layers with mixed group V materials in MBE, usually, special care has to be taken with respect to controlling the interfaces. Similar structures reported in literature often employ special shutter sequences at each interface to minimize the cross incorporation of the group V materials and thereby enhance the quality of the interface.[17–19] These growth interrupts, however, significantly prolong the growth time, e.g., with respect to the sequence described in Ref. 20 by 50% for this sample. For this study, growth interrupts have been omitted completely in order to reduce the total growth time. The processing of the devices starts with the definition of the mesa by lithography and wet-chemical etching with $H_3PO_4$:$H_2O_2$:$H_2O$ (3:4:40). Using the given etching recipe, we observed an etching rate of 5.5 nm/s. In the next step, both bottom and top contacts are defined by lithography, Ti/Au sputtering, and lift-off. Ti/Au is sufficient to produce ohmic contacts even for low doped contact layers because of the large number of surface states of InAs. To measure the spectral response, a Fourier-transform infrared spectrometer was used with a Globar broadband light source. The mesa devices were illuminated through a 45° polished facet. The measured photocurrent spectra at different operation temperatures are shown in Figure 2. We were able to verify that the peak originates from the designed intersubband transition by comparing the photocurrent spectrum for TM and TE polarized incident light. A peak responsivity of 1.9 mA/W for 4.84 $\mu$m was measured at $T = 300$ K.

Another consequence of the lower effective mass is a decrease of the intersubband scattering rates, which determine the extraction efficiency and the resistance of the QCD. The most dominant scattering mechanism for QCDs at temperatures around 300 K is LO-phonon scattering. The scattering rate from one initial state $i$ to another final state $f$ can be calculated by

$$\frac{1}{\tau_{LO}} = \frac{m_e e^2 E_{LO}}{2\hbar^2}(1+n)\left(\frac{1}{\varepsilon_\infty} - \frac{1}{\varepsilon_S}\right) \times \int\int \mathrm{d}z\mathrm{d}z' \psi_f^*(z)\psi_f(z')\psi_i(z)\psi^*(z') \times \int_0^{2\pi} \mathrm{d}\theta \frac{\mathrm{e}^{-Q|z-z'|}}{Q}, \quad (2)$$

where $E_{LO}$ is the LO-phonon energy, $\varepsilon_\infty$ is the high-frequency dielectric constant, $\varepsilon_S$ is the static dielectric constant, $n$ is the temperature dependent LO-phonon population, and $Q$ is given by

$$Q = \left(k_i^2 + k_f^2 - 2k_i k_f \cos\theta\right)^{\frac{1}{2}}, \quad (3)$$

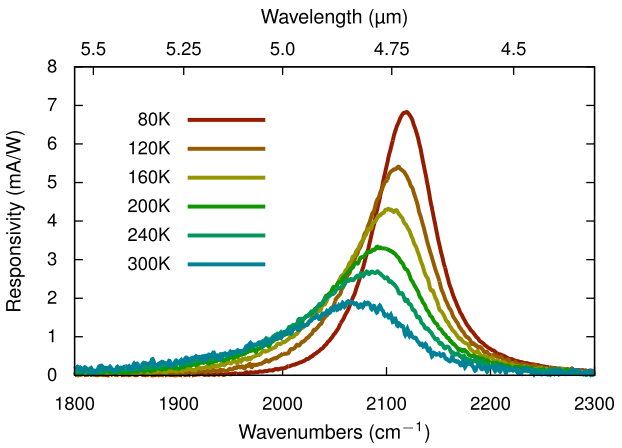


FIG. 2. Measured responsivity spectrum at different temperatures of the InAs/AlAsSb QCD.

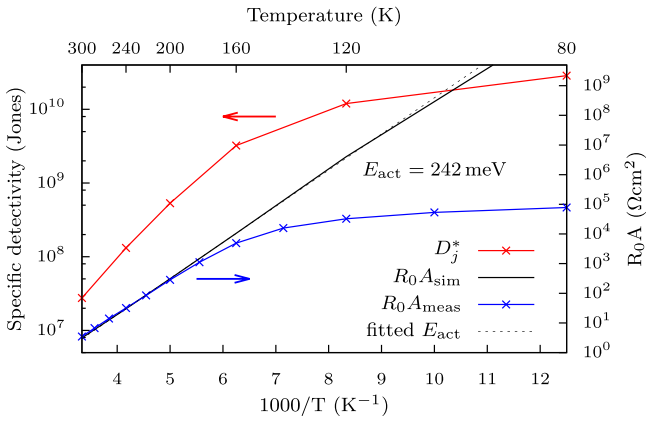


FIG. 3. Arrhenius plot of the specific detectivity (red) and the measured and simulated resistance/area product (blue and black). The extracted activation energy is $E_{act} = 242$ meV.

$$k_f^2 = k_i^2 + \frac{2m^*}{\hbar}(E_i - E_f - E_{LO}), \tag{4}$$

where $k_i$ and $k_f$ are the wavevectors of the initial and final state.[21] As long as there is no bottleneck in the extractor, the extraction efficiency is mostly determined by the ratio between the scattering rate between upper and lower absorption level, and upper absorption level and extractor levels. Since both rates decrease equivalently with a smaller effective mass, the effects cancel out. Still, the reduction of the scattering rates improves the specific detectivity by a reduction of the noise. The dominant noise mechanisms for QCDs are shot noise and Johnson noise.[22] Both can be evaluated by a unified model, where each transition is replaced by a conductor $G$ that can be calculated by

$$4k_bTG = 2e\left(\frac{\rho_i}{\tau_{ij}} + \frac{\rho_j}{\tau_{ji}}\right). \tag{5}$$

The noise spectral density (NSD) per period then given by

$$NSD_{period} = 4k_bTG_{period}, \tag{6}$$

where $\rho_i$ is the carrier population in state $i$, and $\tau_{ij}$ is the scattering time between states $i$ and $j$. The total noise of a QCD is determined by the network of electronic transitions, the amount of carriers, and the scattering rates. Thus, in accordance with Equation (2), the lower effective mass leads to a reduction of the scattering rates, which increases the device resistance and thus further improves the specific detectivity.[23] The measured differential resistance around zero bias and the specific detectivity at different temperatures is shown in Figure 3. A specific detectivity of $2.7 \times 10^7$ Jones is obtained at a temperature of $T = 300$ K.

In conclusion, this work reports on InAs/AlAsSb as material system for QCDs. The material provides a high conduction band offset together with a low effective mass. The conduction band offset shifts the absorption limit to higher energies, while the low effective mass directly increases the absorption coefficient of the QCD material and reduces the noise. This device was optimized for robustness rather than optimum performance and showed a peak responsivity of 1.9 mA/W at a wavelength of $\lambda = 4.84\ \mu$m together with a specific detectivity of approximately $2.7 \times 10^7$ Jones at $T = 300$ K.

The authors acknowledge the support by the Austrian Science Funds (FWF) in the framework of the Doctoral School "Building Solids for Function" (Project No. W1243) and the project IRON (F2503-N17), the PLATON project 35N within the Austrian NANO initiative, and the FP7 EU-project ICARUS. H.D. is an APART Fellow of the Austrian Academy of Sciences.

[1]H. Schneider, C. Schönbein, G. Bihlmann, P. Van Son, and H. Sigg, Appl. Phys. Lett. **70**, 1602 (1997).
[2]H. Schneider and H. C. Liu, *Quantum Well Infrared Photodetectors* (Springer, Berlin, 2006).
[3]M. Graf, G. Scalari, D. Hofstetter, J. Faist, H. Beere, E. Linfield, D. Ritchie, and G. Davies, Appl. Phys. Lett. **84**, 475 (2004).
[4]M. Graf, N. Hoyler, M. Giovannini, J. Faist, and D. Hofstetter, Appl. Phys. Lett. **88**, 241118 (2006).
[5]D. Hofstetter, M. Beck, and J. Faist, Appl. Phys. Lett. **81**, 2683 (2002).
[6]L. Gendron, M. Carras, A. Huynh, V. Ortiz, C. Koeniguer, and V. Berger, Appl. Phys. Lett. **85**, 2824 (2004).
[7]L. Gendron, C. Koeniguer, V. Berger, and X. Marcadet, Appl. Phys. Lett. **86**, 121116 (2005).
[8]F. R. Giorgetta, E. Baumann, M. Graf, Q. Yangi, C. Manz, K. Köhler, H. E. Beere, D. Ritchie, E. Linfield, A. G. Davies, Y. Fedoryshyn, H. Jäckel, M. Fischer, J. Faist, and D. Hofstetter, IEEE J. Quantum Electron. **45**, 1039 (2009).
[9]H. Liu, C. Song, A. SpringThorpe, and J. Cao, Appl. Phys. Lett. **84**, 4068 (2004).
[10]S. Sakr, E. Giraud, A. Dussaigne, M. Tchernycheva, N. Grandjean, and F. H. Julien, Appl. Phys. Lett. **100**, 181103 (2012).
[11]A. P. Ravikumar, T. A. Garcia, J. De Jesus, M. C. Tamargo, and C. F. Gmachl, Appl. Phys. Lett. **105**, 061113 (2014).
[12]P. Reininger, B. Schwarz, H. Detz, D. MacFarland, T. Zederbauer, A. M. Andrews, W. Schrenk, O. Baumgartner, H. Kosina, and G. Strasser, Appl. Phys. Lett. **105**, 091108 (2014).
[13]I. Vurgaftman, J. Meyer, and L. Ram-Mohan, J. Appl. Phys. **89**, 5815 (2001).
[14]P. Reininger, B. Schwarz, A. Harrer, T. Zederbauer, H. Detz, A. M. Andrews, R. Gansch, W. Schrenk, and G. Strasser, Appl. Phys. Lett. **103**, 241103 (2013).
[15]O. Baumgartner, Z. Stanojevic, and H. Kosina, in *SISPAD* (2011), p. 91.
[16]H. Ye, L. Li, R. Hinkey, R. Yang, T. Mishima, J. Keay, M. Santos, and M. Johnson, J. Vac. Sci. Technol., B **31**, 03C135 (2013).
[17]K. Ohtani and H. Ohno, Appl. Phys. Lett. **82**, 1003 (2003).
[18]R. Teissier, D. Barate, A. Vicet, C. Alibert, A. Baranov, X. Marcadet, C. Renard, M. Garcia, C. Sirtori, D. Revin, and J. Cockburn, Appl. Phys. Lett. **85**, 167 (2004).
[19]X. Marcadet, C. Renard, M. Carras, M. Garcia, and J. Massies, Appl. Phys. Lett. **91**, 161104 (2007).
[20]X. Marcadet, C. Becker, M. Garcia, I. Prévot, C. Renard, and C. Sirtori, J. Cryst. Growth **251**, 723 (2003).
[21]R. Ferreira and G. Bastard, Phys. Rev. B **40**, 1074 (1989).
[22]A. Delga, L. Doyennette, M. Carras, V. Trinité, and P. Bois, Appl. Phys. Lett. **102**, 163507 (2013).
[23]A. Delga, M. Carras, L. Doyennette, V. Trinité, A. Nedelcu, and V. Berger, Appl. Phys. Lett. **99**, 252106 (2011).